PHYSICAL REVIEW C VOLUME 8, NUMBER 6 DECEMBER 1973

Fission Cross Sections of Uranium, Thorium, Bismuth, Lead, and Gold Induced by 58- to 100-MeV Alpha Particles

J. Ralarosy, M. Debeauvais, G. Remy, and J. Tripier
Laboratoire de Physique Corpusculaire, Centre de Recherches Nucléaires de Strasbourg, France

R. Stein and D. Huss
Centre Universitaire du Haut-Rhin, Mulhouse, France
(Received 27 June 1973)

The results presented in this paper have been obtained from experiments using a makrofol (a polycarbonate) detector. After a brief description of the experimental technique, values of measured cross sections are given. These values are discussed in comparison with some known results about spallation reactions, referring to reaction cross sections theoretically calculated from optical models.

I. EXPERIMENTAL TECHNIQUE

A. Detection

The following targets are bombarded: (1) uranium and thorium tetrafluoride (2) natural bismuth, lead, and gold. The detection of induced nuclear reaction products is done inside a 4π geometry using the well-known "sandwich" technique[1-8] (Fig. 1). A thin layer (some hundred Å) of the target material is evaporated onto a part of a makrofol foil surface. Above and close to this evaporated layer, a foil similar to the first one is applied. Both foils of 400- or 600-μm total thickness are hard glued together on their whole surface around the target evaporation, except some little apertures necessary for dissolving off the target material and, later on, for etching the tracks. The "sandwich" is exposed perpendicular to its surfaces. With the help of this detector it is possible to visualize the correlated fragment tracks issued from a bombarded nucleus (Fig. 2).

B. Apparatus

The apparatus used for irradiations is composed of (Fig. 3):
(1) A rotating circular plate P disposed perpendicular to the beam and bearing 12 equidistant square apertures disposed along an annulus of the plate. The rotating motion of the plate is driven by an electric motor M so that it is possible to put one or another determined aperture before the beam direction. Before and close to each aperture some thin absorber foils can be set perpendicular to the beam (makrofol foils of 3 to 20 μm) for the purpose of decreasing the particle energy.[2-4]
(2) A box placed before the plate P and containing a set of thick absorbers (50 to 300 μm) to reduce the energy in large steps, a tantalum quick shutter (0.01 sec), to have a precise exposure time, and a quartz crystal used for the alignment and adjustment of the beam profile.
(3) A control board C, connected to the shutter and to the motor. The detector and target to be irradiated are placed directly behind an aperture of the circular plate, perpendicular to the beam direction. The particles issued from the accelerator are collected inside a Faraday cup at a final stage.

C. Experiments

1. Irradiation

The apparatus previously described is connected directly to the output tube of the accelerator; thus the exposure is done inside a secondary vacuum. The axis of the accelerator output tube and that of the Faraday cup must be the same and must pass through the center of the target sample. Tantalum diaphragms of 1 cm^2 are used. Contributions of fission events induced by particles emitted from secondary reactions upon inner surfaces and diaphragms are negligible.

The experiments have been carried out mainly at the Karlsruhe cyclotron (Germany). α particles had 102.5-MeV (±1%) energy when coming out from the accelerator. Before striking the target, this energy was decreased, progressively by means of makrofol absorber sets of increasing thickness. Inside the considered energy range, between 55 and 100 MeV, the specific energy loss of incident particles is practically a linear function of the thickness of the material that has been crossed; it is equal to ~1.2 MeV per 100 μm in makrofol. The energy dispersion introduced by such absorbers, composed only of light elements (H, C, O) is relatively weak and is of the same order as that of the normal distribution of the energy of particles which are coming out of the accelerator.

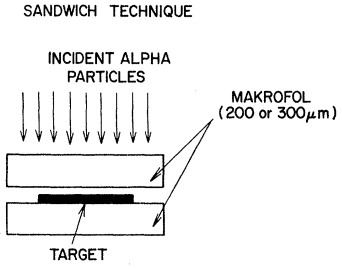

FIG. 1. The sandwich technique.

(This assertion has been justified by using three kinds of detectors: semiconductors, nuclear emulsions, and plastics.) Five values of α-particle energies have been used upon the targets in the range 98, 88, 76, 64, and 58 MeV. Later complementary experiments, carried out at the Grenoble (France) cyclotron (energy lower than 55 MeV), have permitted us to use lower energies. For comparison, we shall reproduce data obtained from these experiments, admitting that interpretations found in the literature are satisfactory.

2. Different Nuclear Interactions Registered

After irradiation, the target is dissolved off and the chemical development of tracks is begun. The reagent is a 5 N NaOH solution, heated to 60°C; the etching time varies between 40 and 90 min.

The "sandwich" technique has a great advantage in studying nuclear interactions. Since phenomena can be registered inside 4π sr, a good number of real parameters are available, and particularly, integrated cross sections can be easily calculated.

Two kinds of phenomena can be registered: on one hand, interactions between the incident particles and the light nuclei of the detector (H, C, O) and on the other hand, interactions between the incident particles and the heavy nuclei of the target. In both cases we must keep in mind that only ion tracks with specific energy losses higher than some critical values can be registered.[1,3,4] Within the energy range we worked on and with the chemical development conditions we used, particles lighter than carbon cannot be visualized and even-

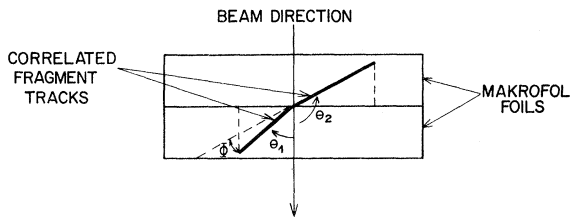

FIG. 2. Correlated fragment tracks.

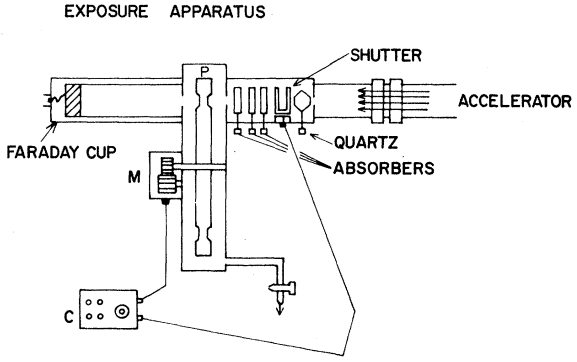

FIG. 3. Exposure apparatus.

tual recoils of nuclei belonging to the target and/or to the detector material leave very short tracks. Fission-fragment ranges are generally longer than 10 μm, whereas visualizable recoil tracks are usually shorter than 2 or 3 μm. Thus, it is very easy to distinguish a fission reaction from other possible reactions, especially since the heavy fragments emitted in fission are visualized in the correlation.

II. RESULTS

Data tables. The values we have obtained are presented in Tables I to V.

Variation curves of cross sections σ_f. The diagrams of Figs. 4 to 7 represent the variations of fission cross sections as a function of the incident energy. We present our measured values and compare them with theoretical values in each of these figures. σ_R represents the (total) reaction cross section calculated from the optical model adapted by Igo and Huizenga[9,10] to incident α particles.

Measurement accuracy. Let us consider an unit surface (1 cm^2) and call n_f the total number of fission events registered, N the number of target nuclei inside the unit surface, N_i the total number of incident particles (integrated during the exposure time). The fission cross section is given by the

TABLE I. $^{238}U + ^{4}He$.

α particle incident energy (MeV)	Target thickness (μg/cm^2)	Quantity of incident charges (nA sec)	Number of observed fission events	Measured cross sections σ_F (b)
98.5±2.0	2.5	4.5	162	2.40±2.00
88.0±1.8	26.0	16.5	5770	2.26±0.34
76.0±1.5	19.4	22.4	5790	2.22±0.40
64.0±1.3	25.7	20.3	6460	2.06±0.32
58.0±1.2	25.7	18.8	5614	1.94±0.30
35.0±0.7	20.1	22.5	3281	1.21±0.22
32.8±0.7	20.1	22.5	3142	1.16±0.21
28.2±0.6	30.1	20.0	1905	0.53±0.08
25.8±0.5	30.1	400.0	581	0.008±0.001

TABLE II. $^{232}Th + ^{4}He$.

α particle incident energy (MeV)	Target thickness ($\mu g/cm^2$)	Quantity of incident charges (nA sec)	Number of observed fission events	Measured cross sections σ_F (b)
98.5 ± 2.0	37.0	3.0	1524	2.25 ± 0.30
88.0 ± 1.8	34.0	21.0	9006	2.07 ± 0.29
76.0 ± 1.5	36.9	20.0	7960	1.77 ± 0.24
64.0 ± 1.3	41.3	21.0	8354	1.58 ± 0.20
58.0 ± 1.2	41.3	24.8	9040	1.45 ± 0.19
32.8 ± 0.7	25.1	21.5	3081	0.93 ± 0.15
30.6 ± 0.6	25.1	21.5	2397	0.73 ± 0.12

following relation:

$$\sigma_f = \frac{n_f}{NN_i},$$

where n_f is obtained by simple counting of correlated events.

We estimate that the relative counting error provided from the scanner is 3%. On the other hand we must take into account the systematical losses of tracks near the horizontal plane which could be etched away during the chemical development and/or absorbed inside the target layer. These systematical losses are of the order of 0.2%, that is to say negligible.

The number N of target nuclei is proportional to the thickness e of the target. The accuracy in the determination of e is 2 $\mu g/cm^2$. The number N_i of incident particles is obtained by measuring the quantity of charges collected throughout the Faraday cup. For incident α particles,

$$N_i = \frac{1}{2}\frac{It}{1.6} \text{ particles},$$

where t is the exposure time and I is the beam intensity.

We estimate that the error in the beam intensity measurement is negligible, but this intensity can be subjected to fluctuations during the exposure time, mainly if I intensity values are weak ($\lesssim 3A$). For all experiments, $\Delta I/I \leq 5\%$. There is practically no error in the exposure time (automatic shutter to 1/100 sec). The errors specified in preceding tables and figures have been calculated from above mentioned estimates.

TABLE III. $^{209}Bi + ^{4}He$.

α particle incident energy (MeV)	Target thickness ($\mu g/cm^2$)	Quantity of incident charges (nA sec)	Number of observed fission events	Measured cross sections σ_F (mb)
98.5 ± 2.0	88.0	10.0	3472	440 ± 45
88.0 ± 1.8	70.2	22.8	5858	400 ± 43
76.0 ± 1.5	50.0	20.3	3058	340 ± 41
64.0 ± 1.3	50.0	22.4	2365	340 ± 29
58.0 ± 1.2	84.0	33.0	5591	220 ± 23
46.5 ± 0.9	110.5	20.0	252	36 ± 4

TABLE IV. $^{207}Pb + ^{4}He$.

α particle incident energy (MeV)	Target thickness ($\mu g/cm^2$)	Quantity of incident charges (nA sec)	Number of observed fission events	Measured cross sections σ_F (mb)
76.0 ± 1.5	74.5	22	2643	180 ± 19
64.0 ± 1.3	74.5	22	1753	120 ± 13
58.0 ± 1.2	86.5	30	1975	93 ± 10

III. DISCUSSION

The cross-section data we have presented agree generally with values given by other authors, when these values exist, as shown in Tables I to V and Figs. 4 to 7. Some authors[11-15] have compared the experimental fission cross section σ_f with the reaction cross section σ_R calculated from the optical model of Igo and Huizenga[9,10]; we shall proceed similarly in the present work.

A. Case of Uranium

The dashed line shown in Fig. 4 represents the variation of the cross section obtained from the square-well model and from the calculations of Blatt and Weisskopf[16] and Shapiro[17] using the following values: $r_0 = 1.5 \times 10^{-13}$ cm for the nucleus and $r_\alpha = 1.2 \times 10^{-13}$ cm for the α-particle radius. All experimental points practically agree with this curve when the error estimates have been taken into account: It does not necessarily signify that fission is the only possible disintegration channel for the presumed previously formed compound nucleus, nor does it signify that fission is wholly issued from a compound nucleus in the considered energy range. In fact, as it has been shown in one of our previous works,[4] a nonnegligible proportion of fission events are due to direct interactions and

TABLE V. $^{197}Au + ^{4}He$.

α particle incident energy (MeV)	Target thickness ($\mu g/cm^2$)	Quantity of incident charges (nA sec)	Number of observed fission events	Measured cross sections σ_F (mb)
98.5 ± 2.0	145	30.0	4255	102 ± 10
88.0 ± 1.8	95	21.4	1677	85 ± 9
76.0 ± 1.5	140	20.3	1514	55 ± 5
64.0 ± 1.3	163	20.3	1081	34 ± 3
58.0 ± 1.2	163	25.2	978	26 ± 3

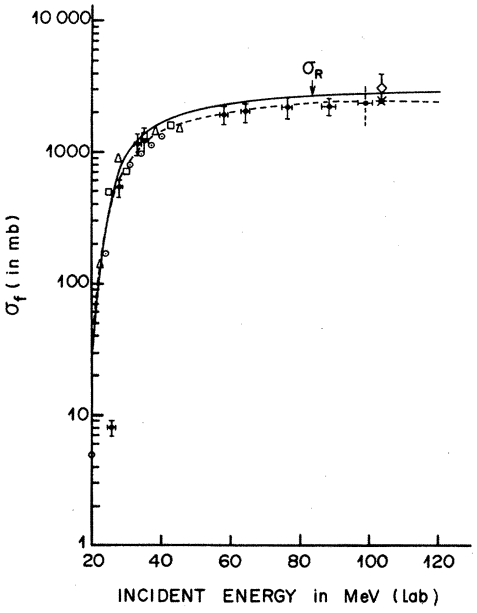

FIG. 4. Uranium fission cross section, $^{238}_{92}U + ^{4}_{2}He$. Dashed line: theoretical curve of Blatt and Weisskopf (Ref. 16) $r_0 = 1.5$ fm; ◇: Ref. 15; ◉: Ref. 11; △: J. Wing, W. J. Rambler, A. L. Harkness, and J. R. Huizenga, Phys. Rev. 114, 163 (1959); □: J. R. Huizenga, R. Vandenbosch, and W. Warhanek, Phys. Rev. 124, 1964 (1961); ⊕: Present work; ✱: Refs. 15 and 14.

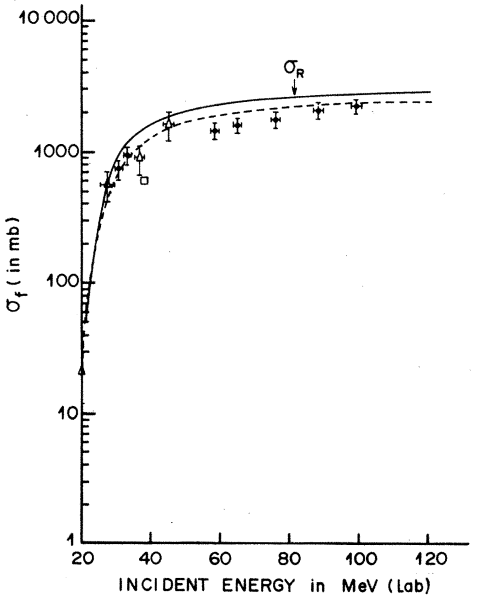

FIG. 5. Thorium fission cross section, $^{232}_{90}Th + ^{4}_{2}He$. Dashed line: Theoretical curve of Blatt and Weisskopf (Ref. 16) $r_0 = 1.5$ fm; △: Ref. 18, B. M. Foreman, UCRL Report No. UCRL-8223 (1958); E. K. Hyde, *The Nuclear Properties of Heavy Elements* (Prentice Hall, New Jersey, 1964), Vol. III.; □: A. S. Newton, Phys. Rev. 75, 17 (1949); ⊕: present work.

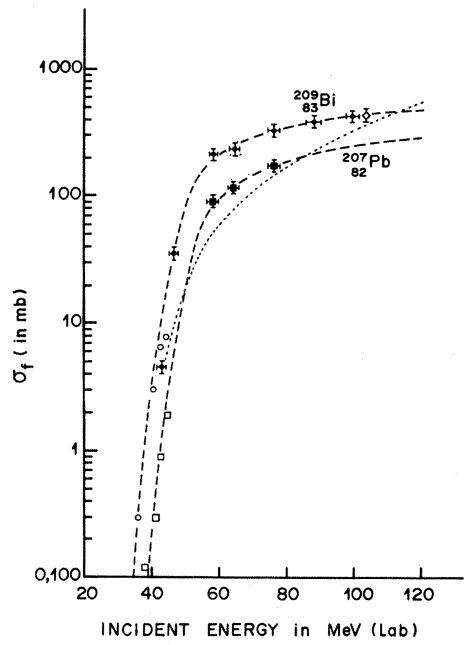

FIG. 6. Lead reaction cross section, Pb + $^{4}_{2}He$. □: J. R. Huizenga, R. Chaudry, and R. Vandenbosch, Phys. Rev. 126, 210 (1962); ⊕: present work; △ and ○: see text.

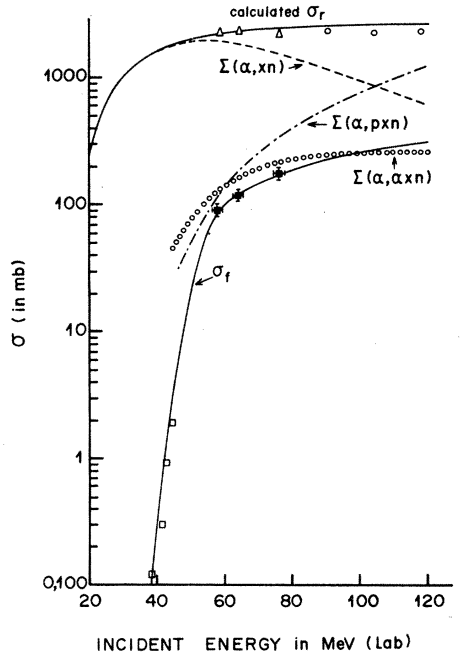

FIG. 7. Bismuth and lead fission cross sections, $^{209}_{83}Bi + ^{4}_{2}He$ and $^{207}_{82}Pb + ^{4}_{2}He$. ^{209}Bi: ◇ : Ref. 15; ○: J. R. Huizenga, R. Chaudry, and R. Vandenbosch, Phys. Rev. 126, 210 (1962); ⊕: present work. ^{207}Pb: □: J. R. Huizenga, R. Chaudry, and R. Vandenbosch, Phys. Rev. 126, 210 (1962); ⊕: present work; dotted line: Ref. 20.

not to compound-nuclear reactions.

The full line curve represents the total reaction cross section σ_R as given by the optical model. It has been plotted from data mentioned in Refs. 9–11, 14, and 15. Although the cross sections we got are systematically below the σ_R curve ($\sigma_f/\sigma_R \simeq 85$ to 95%), the σ_R curve could still account for our data within error limits.

B. Case of Thorium

Experimental results are reproduced in Fig. 5. The dashed line has been plotted from the Blatt and Weisskopf model, with the same values of parameters as previously, whereas the full line represents σ_R.

Our points corresponding to 58, 64, and 76 MeV are below both curves. It is likely to be related to the variations of the spallation-fission competition, as the incident energy varies. Foreman *et al.*,[18] in accord with previous works about spallation-fission competitions at energy ranges lower than 46 MeV have pointed out that (α, xn) reaction products proceed mainly from the deexcitation of compound nuclei and are strongly decreased in proportion by the competition of the fission reaction, whereas other reactions such as $(\alpha, p2n)$ are very likely to be related to noncompound processes and are thus little affected by the fission competition. At the moment we wrote this paper, we had no knowledge of other works about interactions between thorium and α particles at energies higher than 50 MeV. Thus we cannot follow the relative variation of spallation and fission within the energy range considered. Nevertheless, we may suppose that the rates of these variations are the same as those corresponding to a lead target, except for the ordinates. In the next section, upon considering these rates we have taken the liberty of explaining qualitatively the variation of the thorium fission cross section.

C. Case of Lead and Bismuth

The total reaction cross section σ_R can be decomposed mainly into four terms (Fig. 6):

$$\sigma_R = \Sigma(\alpha, xn) + \Sigma(\alpha, pxn) + \Sigma(\alpha, \alpha xn) + \sigma_f .$$

$\Sigma(\alpha, xn)$ increases up to a maximal value and decreases later on when the incoming energy increases. For lead, this maximal value is between 45 and 65 MeV; $\Sigma(\alpha, pxn)$ increases regularly with the increasing incident energy; $\Sigma(\alpha, \alpha xn)$ increases regularly too with increasing incident energy but with much lower slopes than $\Sigma(\alpha, pxn)$ and a little lower slopes than σ_f; σ_f increases with increasing incoming energy, starting very quickly but varying more slowly later on. For lead at 120 MeV, $\Sigma(\alpha, xn) \simeq 600$ mb, $\Sigma(\alpha, pxn) \simeq 1200$ mb, $\Sigma(\alpha, \alpha xn) \simeq 260$ mb, and $\sigma_f \simeq 300$ mb. The first three values are estimated values given in Ref. 19. The σ_f value is a calculated value obtained by an extrapolation of our own results. For extrapolating the lead fission cross-section curve toward higher energies, we have assumed that the variation rates of the lead and the bismuth cross section curves are the same, except for the ordinates. Thus, we have first fitted the data corresponding to bismuth and then the data corresponding to lead in such a way that the rates of both obtained curves are the same.

When spallation and direct interaction reactions are considered together, it would be possible—but a verification must be done—that for thorium, the sum of their cross sections represents precisely a maximal proportion in comparison with fission cross section at energies between 45 and 80 MeV. Thus, the fission reaction would be relatively disadvantaged; so the positions of thorium points corresponding to 58, 64, and 76 MeV (Fig. 5) could be explained.

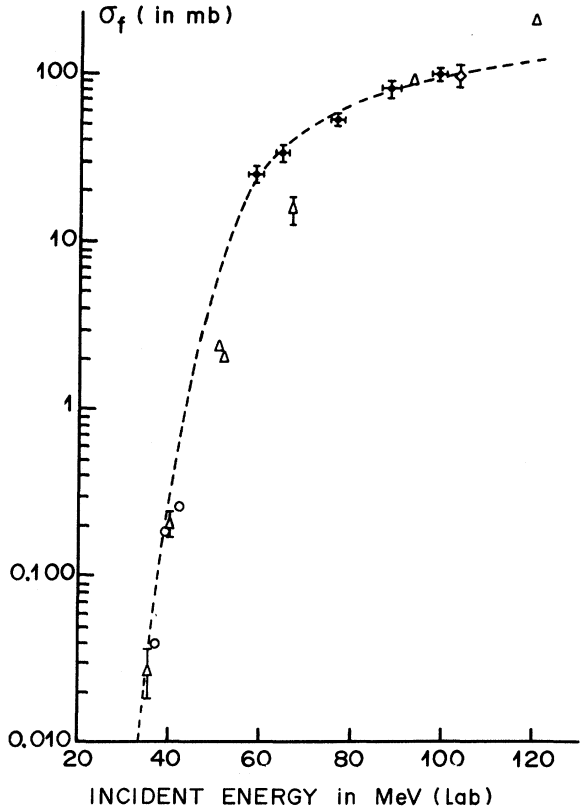

FIG. 8. Gold fission cross section, $^{197}_{79}$Au + $^{4}_{2}$He. ○: J. R. Huizenga, R. Chaudry, and R. Vandenbosch, Phys. Rev. 126, 210 (1962); △: Ref. 13; ⊢●⊣: present work; ◇: Ref. 15.

TABLE VI. σ_f/σ_R(in %).

Target \ Energy (MeV)	43	60	80	100
Bi	0.35 [a]	12	16	20 [a]
Pb	0.09	6	9	12
Au	0.035 [a]	1.2	2.7	4.2 [a]

[a] See also Refs. 15 and 14.

Fission cross sections of bismuth and lead are presented in Fig. 7 at different incident energies. All our points are in good agreement with those given in the literature.

The fission of bismuth and lead induced by α particles has not been frequently studied at energies higher than 45 MeV. Presently, we have only knowledge of a small number of papers, among which we find Refs. 15 and 19–21 interesting. It can be pointed out that our curves corresponding to bismuth agree with the point of Gindler *et al.*[15] at 103 MeV. Khodaĭ-Joopari's[20] data corresponding to lead are plotted and represented by the dotted line, the rate of which is somewhat different from our own curve. Between 50 and 76 MeV his values are lower and become relatively very high when the incident energy increases.

Fairhall, Jensen, and Neuzil[22] have shown that for nuclei of the region of lead, the fissionability depends strongly on the atomic number, whereas it is almost independent of the isotope masses. This indicates that the only consideration of the parameter Z^2/A is insufficient to explain the relative fissionability. Their results have been obtained from incident particles with energies lower than 44 MeV, but we may suppose that their assumption is worthwhile at a higher energy range.

Bimbot *et al.*[19,23] have studied the mechanism of nuclear reactions induced by 60- to 150-MeV α particles upon 206 and 208 lead targets. They have particularly measured the spallation and direct-interaction cross sections. In their discussion about the mechanism, they have compared the sum of the cross sections they obtained and the fission cross section measured by Khodaĭ-Joopari[20] with the reaction cross section calculated from the model of Huizenga and Igo.[10,9] We have proceeded likewise, but our fission cross-section data on the contrary have been summed with the values presented by Bimbot *et al.* Taking into account the previous assumption of Fairhall *et al.*, we have made no difference among the considered lead isotopes. The curves corresponding to the different reactions studied can be seen in Fig. 6. Unfortunately, we could measure fission cross sections for three energies only (58, 64, and 76 MeV); the corresponding summation (triangles) has lead us to values in good agreement with the σ_R curve. At higher energies, we have made summations from three different values chosen on the extrapolated part of the cross-section curve. It can be pointed out that the obtained results are represented (circles) by three values which can be considered within error limits as lined upon σ_R, although they are systematically lower.

D. Case of Gold

The experimental results corresponding to gold are presented in Fig. 8. The curve is drawn by fitting the data. Burnett *et al.*[13] had carried out the same measurements of cross sections up to 120 MeV, using a mica visual detector. Their 66.5-MeV point is below the curve, whereas their 92.9-MeV point such as Gindler's[15] at 103 MeV are in agreement with the curve.

IV. CONCLUSION

It can be pointed out by examining the fission cross section σ_f of the five targets studied that: for uranium, σ_f represents approximately 90% of the reaction cross section σ_R when the incident energy falls within 40 and 90 MeV; for thorium, σ_f/σ_R although close to 1 is a little smaller than for uranium; on the other hand, for the three lighter targets, σ_f is unimportant at 40 MeV, but increases quickly with increasing energy. The lower the atomic number of the target, the lower is the contribution of fission to the reaction cross section. The variation of σ_f/σ_R as a function of the incident energy and as a function of the atomic number of the target is shown in Table VI.

V. ACKNOWLEDGMENTS

This work has been achieved under Professor P. Cüer's direction. We are very grateful to Dr. Katz and Dr. Münzel (Kalsruhe) as well as to Professor Barjon (Grenoble) and Dr. Engelhardt (Karlsruhe-Grenoble) for facilities and help given in exposures. We are indebted to Dr. Bimbot (Orsay) for interesting and profitable discussions. It is a pleasure to acknowledge the careful help offered by our group of technicians.

[1]J. Ralarosy, R. Schmitt, G. Mosinski, J. Tripier, M. Debeauvais, R. Stein, and G. Remy, J. Phys. (Paris) 30, 1 (1969).
[2]J. Ralarosy, M. Debeauvais, R. Stein, G. Remy, and J. Tripier, C. R. Acad. Sci. (Paris) 269, 593 (1969).
[3]J. Ralarosy, J. Tripier, R. Stein, G. Remy, and M. Debeauvais, J. Phys. (Paris) 32, 733 (1971).
[4]J. Ralarosy, thesis, Strasbourg, 1972 (unpublished).
[5]G. Remy, J. Ralarosy, R. Stein, M. Debeauvais, and J. Tripier, J. Phys. (Paris) 31, 27 (1970).
[6]G. Remy, J. Ralarosy, R. Stein, M. Debeauvais, and J. Tripier, Nucl. Phys. A163, 583 (1971).
[7]M. Debeauvais, R. Stein, J. Ralarosy, and P. Cüer, Nucl. Phys. A90, 186 (1967).
[8]M. Debeauvais, R. Stein, G. Remy, and J. Ralarosy, J. Phys. (Paris) Supp. 29, C1–127 (1968).
[9]G. Igo, Phys. Rev. 115, 1665 (1959).
[10]J. R. Huizenga and G. Igo, Nucl. Phys. 29, 462 (1962).
[11]L. T. Colby, Jr., M. L. Shoaff, and J. W. Cobble, Phys. Rev. 121, 1415 (1961).
[12]V. E. Viola, Jr., M. M. Minor, A. E. Salwin, R. O. Bondelid, and R. B. Theus, Nucl. Phys. A174, 321 (1971).
[13]D. S. Burnett, R. C. Gatti, F. Plasil, P. B. Price, W. C. Swiatecki, and S. G. Thompson, Phys. Rev. 134, B952 (1964).
[14]S. S. Kapoor, H. Baba, and S. G. Thompson, Phys. Rev. 149, 965 (1966).
[15]J. Gindler, H. Münzel, J. Buschmann, G. Christaller, F. Michel, and G. Rohde, Nucl. Phys. A145, 337 (1970).
[16]J. M. Blatt and V. F. Weisskopf, *Theoretical Nuclear Physics* (Wiley, New York, 1952).
[17]M. M. Shapiro, Phys. Rev. 90, 171 (1953).
[18]B. M. Foreman, W. M. Gibson, R. A. Glass, and G. T. Seaborg, Phys. Rev. 116, 382 (1959).
[19]R. Bimbot and Y. Le Beyec, J. Phys. (Paris) 32, 243 (1971).
[20]A. Khodaĭ-Joopari, Univ. of California, Lawrence Radiation Laboratory Report No. UCRL 16489, 1966 (unpublished).
[21]F. Plasil, D. S. Burnett, H. C. Britt, and S. G. Thompson, Phys. Rev. 142, 696 (1966).
[22]A. W. Fairhall, R. C. Jensen, and E. F. Neuzil, in *Proceedings of the Second United Nations Conference on the Peaceful Uses of Atomic Energy* (United Nations, Geneva, 1958), Vol. 15, paper No. P/677, p. 1677.
[23]R. Bimbot, H. Jaffrezic, Y. Le Beyec, M. Lefort, and A. Vigny-Simon, J. Phys. (Paris) 30, 513 (1969).